ISSN 1672-9145 **Acta Biochimica et Biophysica Sinica** 2007, **39**(1): 37–45 **CN** 31-1940/Q

Fluorescence Resonance Energy Transfer Analysis of Bid Activation in Living Cells during Ultraviolet-induced Apoptosis

Yinyuan WU, Da XING*, Lei LIU, Tongsheng CHEN, and Wei R. CHEN

MOE Key Laboratory of Laser Life Science & Institute of Laser Life Science, South China Normal University, Guangzhou 510631, China

Abstract Ultraviolet (UV) irradiation is a DNA-damaging agent that triggers apoptosis through both the membrane death receptor and mitochondrial apoptotic signaling pathways. Bid, a pro-apoptotic Bcl-2 family member, is important in most cell types to apoptosis in response to DNA damage. In this study, a recombinant plasmid, YFP-Bid-CFP, comprised of yellow and cyan fluorescent protein and a full length Bid, was used as a fluorescence resonance energy transfer analysis (FRET) probe. Using the FRET technique based on YFP-Bid-CFP, we found that Bid activation was initiated at 9±1 h after UV irradiation, and the average duration of the activation was 75±10 min. Bid activation coincided with a collapse of the mitochondrial membrane potential with an average duration of 50±10 min. When cells were pretreated with Z-IETD-fmk (caspase-8 specific inhibitor) the process of Bid activation was completely inhibited, but the apoptosis was only partially affected. Z-DEVD-fmk (caspase-3 inhibitor) and Z-FA-fmk (non asp specific inhibitor) did not block Bid activation. Furthermore, the endogenous Bid activation with or without Z-IETD-fmk in response to UV irradiation was confirmed by Western blotting. In summary, using the FRET technique, we observed the dynamics of Bid activation during UV-induced apoptosis and found that it was a caspase-8 dependent event.

Key words ultraviolet irradiation; Bid activation; apoptosis; caspase-8; fluorescence resonance energy transfer analysis

Bid was first reported in 1996 and is widely expressed in various tissues, with the highest level in the kidney [1]. In a resting cell, Bid is predominantly cytoplasmic. Following tumor necrosis factor-α (TNF-α) or Fas treatment, Bid is cleaved by caspase-8 in an unstructured loop, exposing a new amino terminal glycine residue, which becomes myristoylated, facilitating its translocation to the mitochondria where it induces the activation of Bax and Bak, resulting in the release of cytochrome c [2,3]. However, the apoptotic pathways in which Bid plays a role are not yet fully characterized. Studies with $Bid^{-/-}$ mice have demonstrated that Bid is required for Fas-induced apoptosis [4]. On the other hand, $Bid^{-/-}$ mouse embryonic fibroblasts (MEFs) were found to be as susceptible as $Bid^{+/+}$ MEFs to a wide range of intrinsic damage signals [5]. Recently, it was demonstrated that $Bid^{-/-}$ MEFs are less susceptible than $Bid^{+/+}$ MEFs to adriamycin, a DNA-damage reagent, as well as to the nucleotide analog 5-fluorouracil [6]. Thus, Bid might contribute to the DNA-damage response.

Ultraviolet (UV) irradiation has multiple cellular targets that trigger different signaling cascades leading to apoptosis. UV irradiation is a DNA-damage agent that activates a p53-dependent apoptotic response [7,8]. DNA damage can change the phosphorylation levels of p53 protein resulting in cell cycle arrest and apoptosis. p53 stimulates a wide network of signals that act through two major apoptotic pathways. The extrinsic pathway is initiated through ligation of the death receptor family receptors by their respective ligands. This family includes the tumor necrosis factor receptors, CD95/Fas/APO-1 and

Received: August 23, 2006 Accepted: November 10, 2006

This work was supported by the grants from the National Natural Science Foundation of China (No. 60378043 and No. 30470494), and the Natural Science Foundation of Guangdong Province (No. 015012, No. 04010394 and No. 2004B10401011)

*Corresponding author: Tel, 86-20-85210089; Fax, 86-20-85216052; E-mail, xingda@scnu.edu.cn

DOI: 10.1111/j.1745-7270.2007.00246.x

the TRAIL receptors [9,10]. Receptor ligation is followed by the formation of the death-inducing signaling complex (DISC), which is composed of the adapter molecule FADD and caspase-8 [11,12]. Recruitment to DISC activates caspase-8, which in turn either directly cleaves and activates the effector caspases, or indirectly activates the downstream caspases through cleavage of the BH3 protein Bid, leading to engagement of the intrinsic pathway of apoptosis [13–16]. The intrinsic pathway of caspase activation is regulated by the pro- and anti-apoptotic Bcl-2 family proteins. These proteins induce or prevent the release of apoptogenic factors, such as cytochrome c and Smac/DIABLO, from the mitochondrial intermembrane space into the cytosol [17–20].

Fluorescence resonance energy transfer (FRET) is a process by which transfer of energy occurs from a donor fluorophore molecule to an acceptor fluorophore molecule in close proximity. The emission spectrum of the donor molecule overlaps with the absorption spectrum of the acceptor molecule. When the two fluorophores are spatially close enough, there is energy transfer between the donor and acceptor molecules. The excited donor transfers its energy to the acceptor, which results in a reduction in donor fluorescence emission and, at the same time, an increase in acceptor fluorescence emission [21]. Thus, FRET is a powerful technique that can provide insight into the spatial and temporal dynamics of protein-protein interactions *in vivo* [22–26]. Recently, a fusion protein YFP-Bid-CFP, which was constructed by connecting cyan fluorescent protein (CFP) and yellow fluorescent protein (YFP) to the C terminus and N terminus of Bid, respectively, has been used to observe the dynamics of Bid activation [27].

In this study, to investigate Bid activation induced by UV irradiation, we transfected ASTC-a-1 cells with YFP-Bid-CFP and examined the dynamics of Bid activation at the single cell level, which was confirmed by fluorescence spectroscopy and Western blotting analysis. Our findings extend the knowledge about the cellular signaling mechanisms mediating UV-induced apoptosis.

Materials and Methods

Materials

Dulbecco's modified Eagle's medium (DMEM) was purchased from Gibco (Grand Island, USA). Z-IETD-fmk (caspase-8 inhibitor), Z-DEVD-fmk (caspase-3 inhibitor) and Z-FA-fmk (non asp specific inhibitor) were purchased from BioVision (Mountain View, USA). Lipofectamine reagent, recombinant human TNF-α and cycloheximide (CHX) were purchased from Invitrogen (Carlsbad, USA). DNA extraction kit was purchased from Qiagen (Valencia, USA). YFP-Bid-CFP was kindly supplied by Dr. K. TAIRA [27]. Other chemicals were mainly from Sigma (St. Louis, USA).

Cell culture and treatment

The human lung adenocarcinoma cell line (ASTC-a-1) was obtained from the Department of Medicine, Jinan University (Guangzhou, China) and cultured in DMEM supplemented with 15% fetal calf serum (FCS), penicillin (100 U/ml) and streptomycin (100 mg/ml) with 5% CO_2 at 37 ºC in a humidified incubator. Transfection was performed with Lipofectamine reagent according to the manufacturer's protocol. The medium was replaced with fresh culture medium after 5 h. Cells were examined 24–48 h after transfection. For the generation of stable cell lines, transfected cells were selected in the presence of G418 (1 mg/ml) for 2 weeks and fluorescent clones were enriched. For 120 mJ/cm^2 UV irradiation, medium was removed, and cells were rinsed with phosphate-buffered saline (PBS) and irradiated, and then medium was restored. Cells were pretreated with Z-IETD-fmk (10 μM), Z-DEVD-fmk (40 μM) and Z-FA-fmk (40 μM) for 1 h respectively before UV irradiation. The inhibitors were kept in the medium throughout the experimental process.

FRET analysis

For analysis of Bid activation, cells were transfected with YFP-Bid-CFP [27], and the dynamics of Bid activation was detected at the single cell level by FRET analysis. FRET was performed on a commercial laser scanning microscope (LSM510/ConfoCor2) combination system (Zeiss, Jena, Germany). For excitation, the 458 nm line of an Ar-ion laser was attenuated with an acousto-optical tunable filter, reflected by a dichroic mirror (main beam splitter HFT458), and focused through a Zeiss Plan-Neofluar 40×/1.3 NA oil DIC objective onto the sample. CFP and YFP (FRET-acceptor) emission was collected through 470–500 nm and 535–595 nm barrier filters, respectively. The quantitative analysis of the fluorescence images was performed using Zeiss Rel3.2 image processing software (Zeiss). After background subtraction, the average fluorescence intensity per pixel was calculated. The onset of Bid activation was defined as the time point at which the YFP/CFP emission ratio irreversibly declined. During control experiments, bleaching of the probe was

negligible.

Performance of acceptor photobleaching

ASTC-a-1 cells transfected with YFP-Bid-CFP were grown on the coverslip of a chamber. The chamber was placed on the stage of the LSM microscope for performance of acceptor photobleaching. The acceptor photobleaching was performed with the highest intensity of 514 nm laser, and the images of YFP and CFP were recorded and processed with Zeiss Rel3.2 image processing software.

Spectrofluorometric analysis of Bid activation induced by UV irradiation in living cells

ASTC-a-1 cells stably expressing YFP-Bid-CFP were grown in DMEM supplemented with 15% FCS for 48 h. Then the cells were treated with UV irradiation at fluence of 120 mJ/cm^2. After 12 h, the cells were immediately transferred into a quartz cuvette, which was then placed inside the sample holder of an LSM510 luminescence spectrometer (PerkinElmer, Boston, USA). The fluorescence emission spectra were obtained by carrying out a spectrum scanning analysis of the luminescence spectrometer. The excitation wavelength was 434±5 nm, the excitation slit was 10 nm, the emission slit was 15 nm and the scanning speed was 200 nm/s. The corresponding background spectra of cell-free culture medium were subtracted.

SDS-PAGE and Western blotting analysis

Twelve hours after UV irradiation, cells were scraped from the dish, washed twice with ice-cold PBS (pH 7.4), and lysed with ice-cold lysis buffer [50 mM Tris-HCl, pH 8.0, 150 mM NaCl, 1% Triton X-100, 100 μg/ml phenylmethylsulphonyl fluoride (PMSF)] for 30 min on ice. The lysates were centrifuged at 13,400 *g* for 5 min at 4 ºC, and the protein concentration was determined. Equivalent samples (30 μg protein extract) underwent 12% SDS-PAGE. The proteins were then transferred onto nitrocellulose membranes, and probed with Bid monoclonal antibody (Cell Signaling Technology, Beverly, USA) followed by rabbit primary antibodies conjugated to horseradish peroxidase (KPL, Gaithersburg, USA).

Confirmation of cell apoptosis

ASTC-a-1 cells were cultured in a 96-well microplate at a density of 5×10^3 cells/well for 24 h. The cells were then divided into five groups and exposed to UV irradiation at fluences of 0 (control), 30, 60, 120 and 240 mJ/cm^2 for 12 h respectively. Cell cytotoxicity was assessed with CCK-8 (Dojindo Laboratories, Kumamoto, Japan) according to the manufacturer's instructions. A_{450}, the absorbance value at 450 nm, was read with a 96-well plate reader (DG5032; Huadong, Nanjing, China), and the A_{450} was inversely proportional to the degree of cell apoptosis.

To assess the changes in nuclear morphology typical of apoptosis, ASTC-a-1 cells were cultured on 35 mm glass-bottomed dishes. After 12 h UV irradiation, the cells were washed twice with PBS (pH 7.4). Subsequently, the cells were stained with 1 mM Hoechst 33258 for 10 min at room temperature. The cells were then washed twice with PBS and viewed under a Nikon fluorescent microscope with a 330–380 nm band pass excitation filter and a 450–490 nm band pass emission filter.

Statistical analysis

Data are represented as mean±SEM. Statistical analysis was carried out with Student's paired *t*-test. Differences were considered statistically significant at $P<0.05$.

Results

Characterization of YFP-Bid-CFP in living ASTC-a-1 cells

Bid activation was monitored by the FRET technique using a fusion protein YFP-Bid-CFP, which was comprised of YFP, CFP and the FL-Bid protein as a linker.

Before Bid was activated, CFP and YFP were covalently linked together. Energy could be transferred directly from CFP to YFP, so fluorescence emitted from YFP could be detected when CFP was excited. Once Bid was activated, CFP was separated from YFP, so the FRET effect of YFP-Bid-CFP must have decreased effectively [**Fig. 1(A)**]. Acceptor bleaching experiments were carried out to assess the sensitivity of the FRET probe. Acceptor photobleaching, one of the techniques for measuring FRET, the acceptor molecule of the FRET pair was bleached, resulting in an unquenching of the donor fluorescence [28]. The acceptor fluorophore YFP was selectively bleached by repeated scanning of the cell area [**Fig. 1(B)**]. A quantitative analysis of acceptor bleaching showed the absolute fluorescence intensities for CFP and YFP for a single cell when plotted as a function of time [**Fig. 1(B)**]. On bleaching, there was a marked decrease in the acceptor fluorescence (YFP), which coincided with an increase in the donor fluorescence (CFP) because of an inability of the acceptor to accept energy from the donor after bleaching. Out of the bleaching area, the intensities of CFP and YFP remained unchanged (data not shown). Therefore, the increase of CFP fluo-

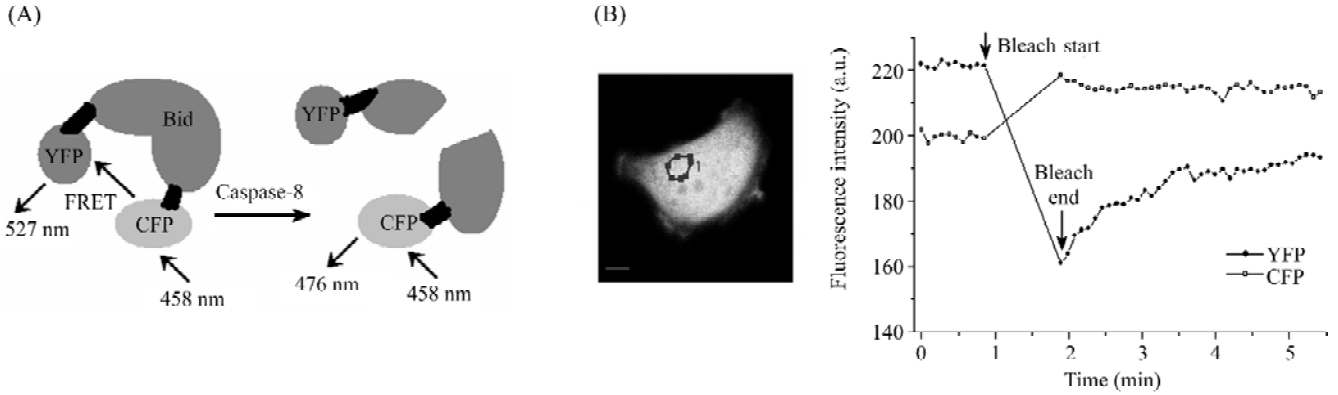

Fig. 1 Characterization of YFP-Bid-CFP in ASTC-a-1 cells

(A) In our FRET analysis system, excitation of CFP at 458 nm should result in emission at 476 nm if no YFP is in close proximity. In the YFP-Bid-CFP, energy should be transferred from excited CFP to YFP, with resulting emission at 527 nm. When the fusion protein is cleaved by caspase-8, YFP is no longer in close proximity to CFP, resulting in YFP decrease and concomitant CFP fluorescence increase. (B) Acceptor photobleaching confirms FRET between CFP and YFP. When YFP was selectively bleached by repeated scanning of the cell area at a high laser power of 514 nm, the intensity of YFP decreased, while the intensity of CFP increased. Scale bar=5 μm.

rescence by bleaching YFP confirmed that FRET exists between the two fluorescent proteins in the YFP-Bid-CFP *in vivo*.

Real-time monitoring of Bid activation during TNF-α-induced apoptosis in living ASTC-a-1 cells

To define our system, we investigated Bid activation during TNF-α-induced apoptosis. Cells were treated with 200 ng/ml TNF-α and 1 μg/ml CHX at the start of the measurement. After 4 h and 55 min, the fluorescence intensity of CFP increased and that of YFP decreased, which implied that YFP-Bid-CFP was cleaved. The typical time-course images of YFP-Bid-CFP are shown in **Fig. 2 (A)**. The same FRET was confirmed by quantitative analysis of fluorescence intensities [**Fig. 2(B)**].

Real-time monitoring of Bid activation during UV-induced apoptosis in living ASTC-a-1 cells

To directly observe the activation of Bid during UV-induced apoptosis, we transfected ASTC-a-1 cells with YFP-Bid-CFP, and then examined the dynamics of Bid activation induced by UV irradiation at the single cell level. The fluorescence intensity of CFP increased and YFP decreased at 9 h after UV irradiation, which implied that

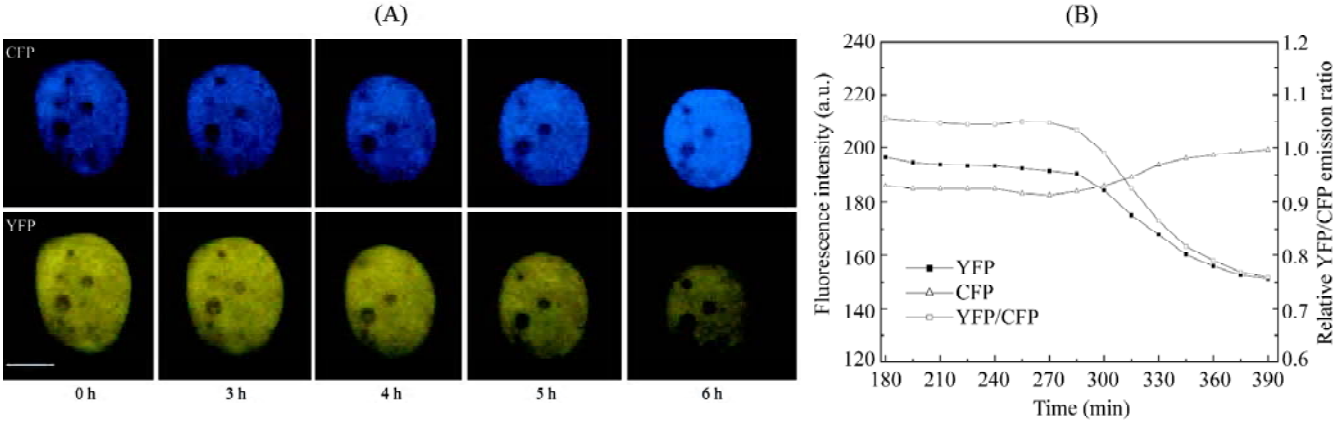

Fig. 2 Dynamics of Bid activation during TNF-α-induced apoptosis in living cells

(A) Dynamics of YFP/CFP ratio images of a typical cell transfected with YFP-Bid-CFP. Scale bar=10 μm. (B) The intensities of CFP emission, YFP emission and YFP/CFP ratio correspond to the data in (A). Similar results were obtained from three separate experiments.

YFP-Bid-CFP was cleaved. The typical time-course images of YFP-Bid-CFP are shown in **Fig. 3(A)**. The imaging analysis commenced 8 h after UV irradiation, and the results showed that Bid activation was initiated at 9 h after UV irradiation and reached its maximum activation in 1 h [**Fig. 3(B)**]. To define the average initiation and duration of Bid activation, we compared the dynamics of Bid activation in four individual cells during UV-induced apoptosis. On

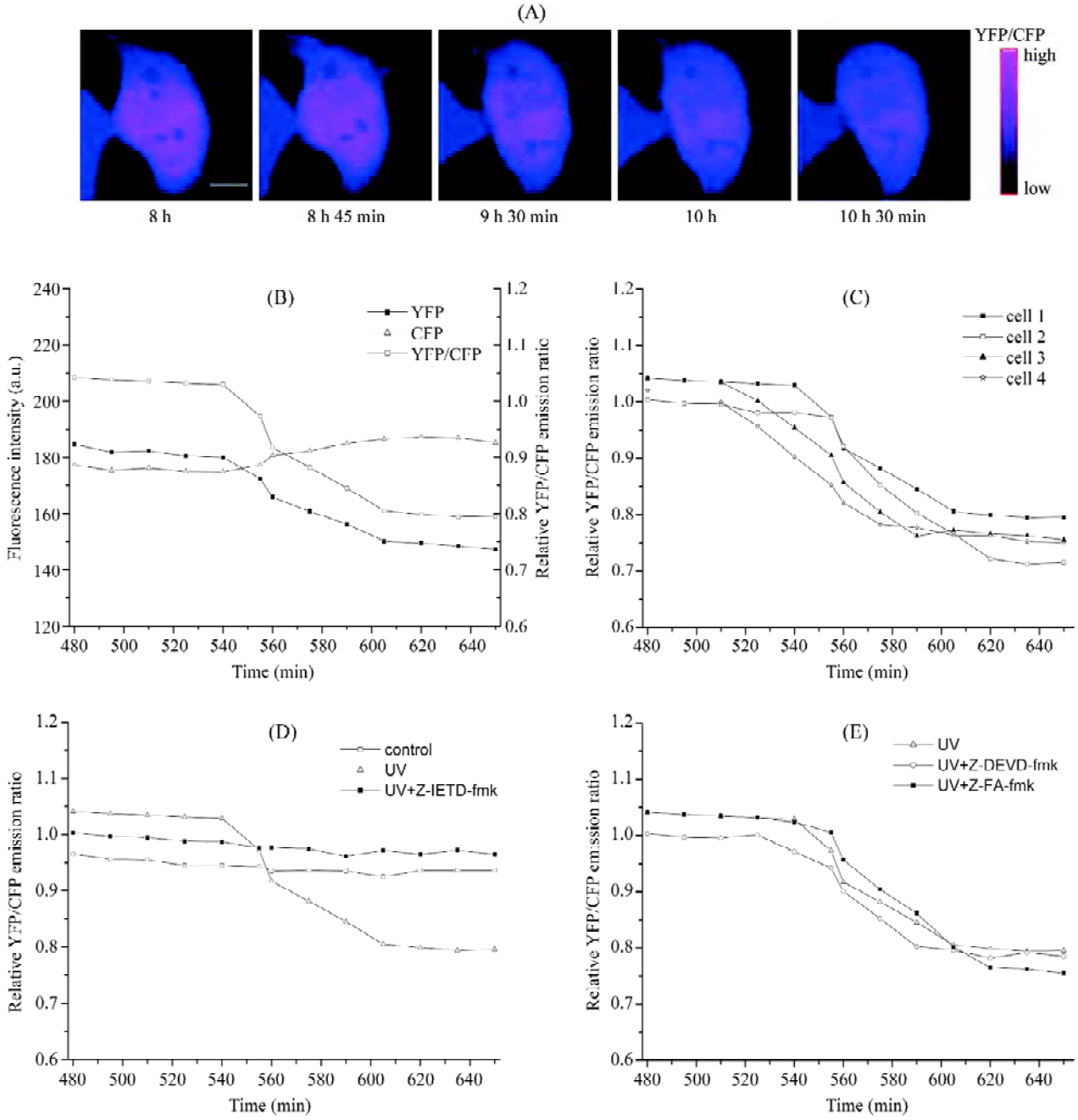

Fig. 3 Dynamics of Bid activation during UV-induced apoptosis in living cells

(A) Dynamics of YFP/CFP ratio images of a typical cell transfected with YFP-Bid-CFP. Imaging analysis was commenced 8 h after UV irradiation. Scale bar=10 μm. (B) Dynamics of CFP emission intensity, YFP emission intensity and YFP/CFP ratio correspond to the data in (A). (C) Dynamics of YFP/CFP ratio for four individual cells after UV irradiation. (D–E) Dynamics of YFP/CFP ratio for cells after different treatments as indicated. The ratio was processed with the same method as (B). Similar results were obtained from three separate experiments.

average, the initiation of Bid activation was 9±1 h after UV irradiation, and the duration of Bid activation was 75±10 min [**Fig. 3(C)**].

To determine whether Bid activation induced by UV irradiation was a caspase-8 dependent event, cells were pretreated with various inhibitors for 1 h before UV irradiation. In the presence of Z-IETD-fmk, the fluorescence intensities of YFP, CFP and the ratio YFP/CFP remained unchanged, which indicated that Bid activation was blocked by inhibiting caspases-8 activation [**Fig. 3 (D)**]. In the samples treated with Z-DEVD-fmk and Z-FA-fmk, the results were the same as that of UV treated cells respectively, which indicated that Z-DEVD-fmk and Z-FA-fmk did not block Bid activation [**Fig. 3(E)**]. These results revealed that the Bid activation was a caspase-8 dependent event.

Real-time detection of a collapse of the mitochondrial membrane potential induced by UV irradiation in living cells

To determine whether Bid activation coincided with a collapse of mitochondrial transmembrane potential induced by UV irradiation, we monitored a collapse of mitochondrial membrane potential using Rhodamine 123. The typical time-course images of Rhodamine 123 are shown in **Fig. 4(A)**. The same results were confirmed by quantitative analysis of fluorescence intensities in three individual cells [**Fig. 4 (B)**]. On average, the initiation of a collapse of mitochondrial transmembrane potential was 540±30 min after UV irradiation, and the duration of a collapse of mitochondrial transmembrane potential was 50±10 min.

Spectrofluorometric and Western blotting analysis of Bid activation induced by UV irradiation in living cells

To further demonstrate Bid activation induced by UV irradiation, we used a spectrometer to measure the changes of FRET effects of YFP-Bid-CFP in response to different treatments as indicated. The results of spectrofluorometric analysis of the activation of YFP-Bid-CFP in living cells are shown in **Fig. 5(A)**. UV irradiation resulted in a decrease in FRET, which indicated that Bid was activated, thus the emission peak of CFP (476 nm) increased, and the emission peak of YFP (527 nm) decreased; and we did not detect such results with UV irradiation in the presence of Z-IETD-fmk. These results further confirmed that Bid activation was a caspase-8 dependent event, which were consistent with the results from single cell imaging analysis.

To find whether the endogenous Bid activation was the same as overexpression, we used Western blotting analysis to study the endogenous Bid activation during UV-induced apoptosis with or without Z-IETD-fmk treatment [**Fig. 5 (B)**]. In the experiment, we used actin as a loading control. In the absence of Z-IETD-fmk, cleaved Bid was detected 12 h after UV irradiation, in the presence of Z-IETD-fmk, cleaved Bid was not detected 12 h after UV irradiation. Thus, it suggested that Bid activation by UV irradiation was a caspase-8 dependent event. The experiments were repeated three times.

UV irradiation induces apoptosis in ASTC-a-1 cells

To establish a proper UV irradiation dose to induce apoptosis, ASTC-a-1 cells were irradiated with various kinds of fluence. Apoptosis was analyzed using a Cell

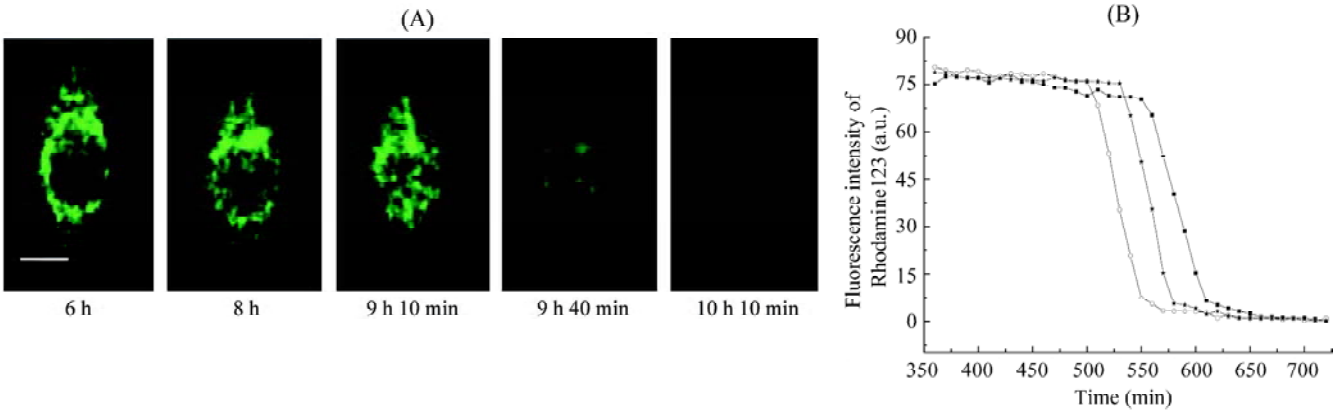

Fig. 4 Real-time detection of collapse of the mitochondrial membrane potential induced by UV irradiation

(A) The typical time-course images of Rhodamine 123 after UV irradiation. Scale bar=10 μm. (B) Quantitative analysis of fluorescence intensities of Rhodamine 123 in three individual cells after UV irradiation. Similar results were obtained from three separate experiments.

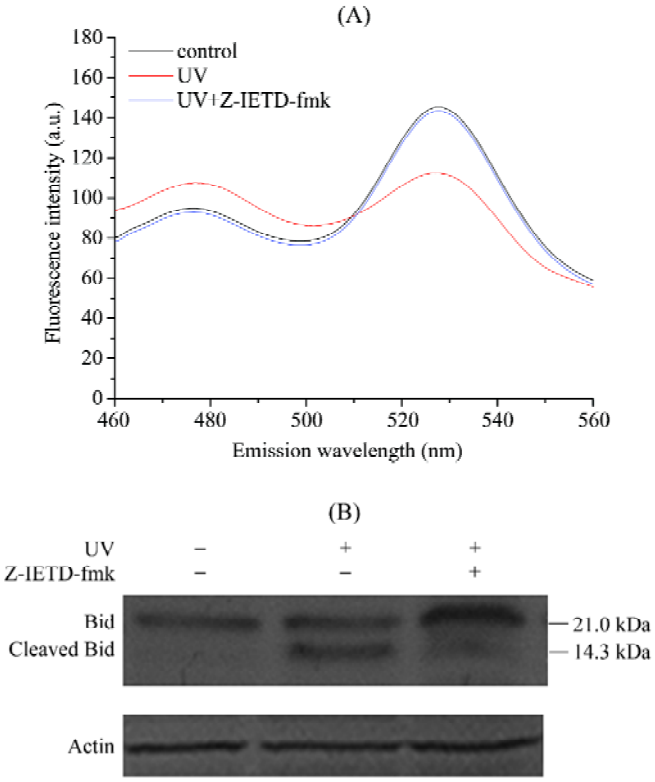

Fig. 5 Spectrofluorometric and Western blotting analysis of Bid activation induced by UV irradiation

(A) Emission spectra of YFP-Bid-CFP 12 h after different treatments as indicated. ASTC-a-1 cells stably expressing YFP-Bid-CFP were excited at the excitation wavelength of CFP (434±5 nm), which resulted in a CFP emission peak (476 nm) and YFP emission peak (527 nm) caused by FRET from CFP. (B) Western blotting analysis of Bid activation by UV irradiation. Actin was used as a loading control. Similar results were obtained from three separate experiments.

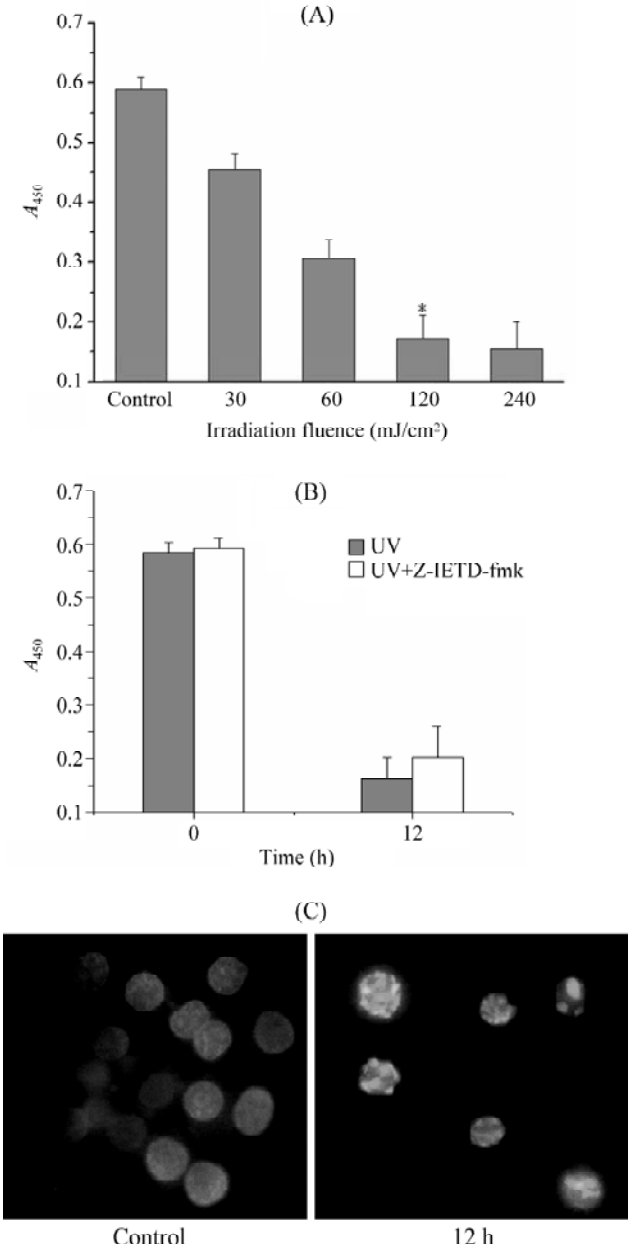

Fig. 6 UV irradiation induces apoptosis in ASTC-a-1 cells

(A) Changes in cell viability induced by UV irradiation. ASTC-a-1 cells were seeded on 96-well microplates for 24 h and then irradiated with UV at a fluence of 0, 30, 60, 120 and 240 mJ/cm², respectively. $^*P<0.05$ vs. control. (B) Changes in cell viability induced by 120 mJ/cm² UV irradiation in the presence of Z-IETD-fmk. Cell viability was assessed by the CCK-8 assay at 12 h after UV irradiation. (C) Hoechst 33258 staining of cells at 12 h after 120 mJ/cm² UV irradiation.

counting kit-8 at 12 h after UV irradiation. The A_{450} value, an indicator of cell apoptosis, was measured. As shown in **Fig. 6(A)**, the A_{450} value decreased as the irradiation fluence increased. This indicated that UV irradiation caused a dose-dependent increase in the percentage of apoptotic cells. A dose of 120 mJ/cm² can induce a substantial number of cells at 12 h after UV irradiation, and at the higher dose of 240 mJ/cm², the percentage of apoptotic cells decreases slightly.

To determine whether Bid activation is required for UV-induced apoptosis or simply activated as a consequence of apoptosis, cell apoptosis was analyzed using a Cell counting kit-8 at 12 h after 120 mJ/cm² UV irradiation in the presence or absence of Z-IETD-fmk, respectively. **Fig. 6 (B)** indicates that Bid did not contribute to UV-induced apoptosis.

To further confirm UV-induced apoptosis, we used Hoechst 33258 staining to observe cells at 12 h after 120 mJ/cm² UV irradiation. As shown in **Fig. 6(C)**, cells exhibited typical apoptotic nuclei at 12 h after UV irradiation judged by chromatin condensation and nuclear fragmentation.

Discussion

UV irradiation is known to induce a cell death cascade involving mitochondria, which eventually leads to apoptosis. However, the precise initiating apoptotic mechanisms upstream of mitochondria remain obscure. Bid activation can be conducted by several proteases. Caspase-8 has been shown to be the major protease responsible for Bid activation during death receptor-mediated apoptosis [13,15], and calpain is also shown to cleave Bid [29,30]. Other reports demonstrate that Bid also can be cleaved by caspase-3 and caspase-2 in the intrinsic pathway, which is independent of death receptors [31–33]. To determine which protease contributes to Bid activation during UV-induced apoptosis, we investigated Bid activation in the presence of Z-IETD-fmk, Z-DEVD-fmk and Z-FA-fmk after UV irradiation. In this study, we monitored for the first time the dynamics of Bid activation during UV-induced apoptosis in living cells. Our results show that the effects of UV irradiation on the ASTC-a-1 cells apoptosis depend on the dose of UV irradiation [**Fig. 6(A)**]. We also show that Z-IETD-fmk did not block UV-induced apoptosis [**Fig. 6 (B)**]. When the cells were treated with UV irradiation (120 mJ/cm^2), a typical dosage of UV irradiation to induce apoptosis of ASTC-a-1 cells in our conditions (**Fig. 6**), both FRET imaging and spectrofluorometric analysis showed an increase in the CFP emission and a corresponding decrease in the YFP emission. However, in the presence of Z-IETD-fmk, there was no change in the CFP and YFP emission (**Figs. 3** and **5**). To further confirm these points, we used Western blotting analysis to study the endogenous Bid activation during UV-induced apoptosis with or without Z-IETD-fmk treatment [**Fig. 5(B)**], and the results were consistent with FRET imaging and spectrofluorometric analysis. In addition, we investigated collapse of mitochondrial transmembrane potential induced by UV irradiation, which coincided with Bid activation (**Fig. 4**).

FRET, a noninvasive technique, can spatio-temporally monitor cellular events in different physiological conditions at a single cell level [34–36]. It has been used to study enzyme activity, protein location, protein translocation, small ligand binding, protein-protein interaction, conformational change, and real-time post-translational modification [22]. Specifically, FRET has been used to detect apoptotic signals that involve activation of different caspases [37–39], interactions between Bcl-2 and Bax [35,40], Ca^{2+} levels [36,41,42] and other protein activities. This can not be fully elucidated by traditional biophysical or biochemical approaches, which can only measure the average behavior of cell populations and the static spatial information available from fixed cells and thus, can not provide direct access to cells life events in their natural environment [22].

In our current study, we employed single-cell FRET analysis to monitor the dynamics of Bid activation by UV irradiation. To our best knowledge, this was the first time that the temporal and spatial profiles of UV-induced apoptosis have been observed by FRET using YFP-Bid-CFP at the single cell level. Our results demonstrated that Bid activation was initiated 9±1 h after UV irradiation, and the average duration of the activation was 75±10 min, which coincided with a collapse of the mitochondrial membrane potential, and Bid activation was a caspase-8 dependent event during UV-induced apoptosis.

Acknowledgement

We thank Dr. TAIRA (University of Tokyo, Tokyo, Japan) for kindly providing the YFP-Bid-CFP plasmid.

References

1 Wang K, Yin XM, Chao DT, Milliman CL, Korsmeyer SJ. BID: A novel BH3 domain-only death agonist. Genes Dev 1996, 10: 2859–2869
2 Zha J, Weiler S, Oh KJ, Wei MC, Korsmeyer SJ. Posttranslational N-myristoylation of BID as a molecular switch for targeting mitochondria and apoptosis. Science 2000, 290: 1761–1765
3 Wang X. The expanding role of mitochondria in apoptosis. Genes Dev 2001, 15: 2922–2933
4 Yin XM, Wang K, Gross A, Zhao Y, Zinkel S, Klocke B, Roth KA *et al*. Bid-deficient mice are resistant to Fas-induced hepatocellular apoptosis. Nature 1999, 400: 886–891
5 Wei MC, Zong WX, Cheng EH, Lindsten T, Panoutsakopoulou V, Ross AJ, Roth KA *et al*. Proapoptotic BAX and BAK: A requisite gateway to mitochondrial dysfunction and death. Science 2001, 292: 727–730
6 Sax JK, Fei P, Murphy ME, Bernhard E, Korsmeyer SJ, El-Deiry WS. BID regulation by p53 contributes to chemosensitivity. Nat Cell Biol 2002, 4: 842–849
7 Kraemer KH. Sunlight and skin cancer: Another link revealed. Proc Natl Acad Sci USA 1997, 94: 11–14
8 ZieglerA, Jonason AS, Leffell DJ, Simon JA, Sharma HW, Kimmelman J, Remington L *et al*. Sunburn and p53 in the onset of skin cancer. Nature 1994, 372: 773–776
9 Locksley R, Killeen N, Lenardo M. The TNF and TNF receptor superfamilies: Integrating mammalian biology. Cell 2001, 104: 487–501
10 Haupt S, Berger M, Goldberg Z, Haupt Y. Apoptosis—the p53 network. J Cell Sci 2003, 116: 4077–4085
11 Boldin MP, Goncharov TM, Goltsev YV, Wallach D. Involvement of MACH, a novel MORT1/FADD-interacting protease, in Fas/APO-1- and TNF receptor-induced cell death. Cell 1996, 85: 803–815
12 Muzio M, Chinnaiyan AM, Kischkel FC, O'Rourke K, Shevchenko A, Ni J, Scaffidi C *et al*. FLICE, a novel FADD-homologous ICE/CED-3-like protease,

is recruited to the CD95 (Fas/APO-1) death inducing signaling complex. Cell 1996, 85: 817–827

13 Luo X, Budihardjo I, Zou H, Slaughter C, Wang X. Bid, a Bcl2 interacting protein, mediates cytochrome c release from mitochondria in response to activation of cell surface death receptors. Cell 1998, 94: 481–490

14 Li H, Zhu H, Xu CJ, Yuan J. Cleavage of BID by caspase 8 mediates the mitochondrial damage in the Fas pathway of apoptosis. Cell 1998, 94: 491–501

15 Gross A, Yin XM, Wang K, Wei MC, Jockel J, Milliman C, Erdjument-Bromage H *et al*. Caspase cleaved BID targets mitochondria and is required for cytochrome c release, while BCL-XL prevents this release but not tumor necrosis factor-R1/Fas death. J Biol Chem 1999, 274: 1156–1163

16 Scaffidi C, Fulda S, Srinivasan A, Friesen C, Li F, Tomaselli KJ, Debatin KM *et al*. Two CD95 (APO-1/Fas) signaling pathways. EMBO J 1998, 17: 1675–1687

17 Kluck RM, Bossy-Wetzel E, Green DR, Newmeyer DD. The release of cytochrome c from mitochondria: A primary site for Bcl-2 regulation of apoptosis. Science 1997, 275: 1132–1136

18 Yang J, Liu X, Bhalla K, Kim CN, Ibrado AM, Cai J, Peng TI *et al*. Prevention of apoptosis by Bcl-2: Release of cytochrome c from mitochondria blocked. Science 1997, 275: 1129–1132

19 Jurgensmeier JM, Xie Z, Deveraux Q, Ellerby L, Bredesen D, Reed JC. Bax directly induces release of cytochrome c from isolated mitochondria. Proc Natl Acad Sci USA 1998, 95: 4997–5002

20 Finucane DM, Bossy-Wetzel E, Waterhouse NJ, Cotter TG, Green DR. Bax-induced caspase activation and apoptosis via cytochrome c release from mitochondria is inhibitable by Bcl-xL. J Biol Chem 1999, 274: 2225–2233

21 Fields S. A novel genetic system to detect protein-protein interactions. Nature 1989, 340: 245–246

22 Gaits F, Hahn K. Shedding light on cell signaling: Interpretation of FRET biosensors. Sci STKE 2003, 165: 1–5

23 Takemoto K, Nagai T, Miyawaki A, Miura M. Spatio-temporal activation of caspase revealed by indicator that is insensitive to environmental effects. J Cell Biol 2003, 160: 235–243

24 Wang F, Chen TS, Xing D, Wang JJ, Wu YX. Measuring dynamics of caspase-3 activity in living cells using FRET technique during apoptosis induced by high fluence low-power laser irradiation. Lasers Surg Med 2005, 36: 2–7

25 Wu Y, Xing D, Chen WR. Single cell FRET imaging for determination of pathway of tumor cell apoptosis induced by photofrin-PDT. Cell Cycle 2006, 5: 729–734

26 Gao X, Chen T, Xing D, Wang F, Pei Y, Wei X. Single cell analysis of PKC activation during proliferation and apoptosis induced by laser irradiation. J Cell Physiol 2006, 206: 441–448

27 Onuki R, Nagasaki A, Kawasaki H, Baba T, Uyeda TQ, Taira K. Confirmation by FRET in individual living cells of the absence of significant amyloid β-mediated caspase 8 activation. Proc Natl Acad Sci USA 2002, 99: 14716–14721

28 Van Munster EB, Kremers GJ, Adjobo-Hermans MJ, Gadella TW Jr. Fluorescence resonance energy transfer (FRET) measurement by gradual acceptor photobleaching. J Microsc 2005, 218: 253–262

29 Vindis C, Elbaz M, Escargueil-Blanc I, Auge N, Heniquez A, Thiers JC, Negre-Salvayre A *et al*. Two distinct calcium-dependent mitochondrial pathways are involved in oxidized LDL-induced apoptosis. Arterioscler Thromb Vasc Biol 2005, 25: 639–645

30 Chen M, Won DJ, Krajewski S, Gottlieb RA. Calpain and mitochondria in ischemia/reperfusion injury. J Biol Chem 2002, 277: 29181–29186

31 Orrenius S, Zhivotovsky B, Nicotera P. Regulation of cell death: The calcium-apoptosis link. Nat Rev Mol Cell Biol 2003, 4: 552–565

32 Bossy-Wetzel E, Green DR. Caspases induce cytochrome c release from mitochondria by activating cytosolic factors. J Biol Chem 1999, 274: 17484–17490

33 Slee EA, Keogh SA, Martin SJ. Cleavage of BID during cytotoxic drug and UV radiation-induced apoptosis occurs downstream of the point of Bcl-2 action and is catalysed by caspase-3: A potential feedback loop for amplification of apoptosis-associated mitochondrial cytochrome c release. Cell Death Differ 2000, 7: 556–565

34 Mahajan NP, Linder K, Berry G, Gordon GW, Heim R, Herman B. Bcl-2 and Bax interactions in mitochondria probed with green fluorescent protein and fluorescence resonance energy transfer. Nat Biotechnol 1998, 16: 547–552

35 Miyawaki A, Llopis J, Heim R, McCaffery JM, Adams JA, Ikura M, Tsien RY. Fluorescent indicators for Ca^{2+} based on green fluorescent proteins and calmodulin. Nature 1997, 388: 882–887

36 Mizuno H, Sawano A, Eli P, Hama H, Miyawaki A. Red fluorescent protein from *Discosoma* as a fusion tag and a partner for fluorescence resonance energy transfer. Biochemistry 2001, 40: 2502–2510

37 Takemoto K, Nagai T, Miyawaki A, Miura M. Spatio-temporal activation of caspase revealed by indicator that is insensitive to environmental effects. J Cell Biol 2003, 160: 235–243

38 Rehm M, Dussmann H, Janicke RU, Tavare JM, Kogel D, Prehn JH. Single-cell fluorescence resonance energy transfer analysis demonstrates that caspase activation during apoptosis is a rapid process. J Biol Chem 2002, 227: 24506–24514

39 Thorburn J, Bender LM, Morgan MJ, Thorburn A. Caspase-and serine protease-dependent apoptosis by the death domain of FADD in normal epithelial cells. Mol Biol Cell 2003, 14: 67–77

40 Mahajan NP, Linder K, Berry G, Gordon GW, Heim R, Herman B. Bcl-2 and Bax interactions in mitochondria probed with green fluorescent protein and fluorescence resonance energy transfer. Nat Biotechnol 1998, 16: 547–552

41 Miyawaki A, Griesbeck O, Heim R, Tsien RY. Dynamic and quantitative Ca^{2+} measurements using improved cameleons. Proc Natl Acad Sci USA 1999, 96: 2135–2140

42 Miyawaki A, Tsien RY. Monitoring protein conformations and interactions by fluorescence resonance energy transfer between mutants of green fluorescent protein. Methods Enzymol 2000, 327: 472–500

Edite by
Xianxi WANG